DEVELOPMENT OF ENCLOSURE FIRE MODEL INCORPORATING PYROLYSIS OF WOOD AND PREDICTION OF FLASHOVER

R.K.K. Yuen
Fire Safety and Disaster Prevention Research Group
Department of Building and Construction, City University of Hong Kong, Hong Kong

ABSTRACT

Flame spread and fire over cellulosic materials occur when the burning region supplies sufficient heat to the virgin solid to cause gasification. Under proper conditions, the reaction between the generated volatiles and the oxidant (air) may be sustained. The characteristics of the flame spread are therefore the result of heat and mass transfer processes as well as finite-rate gas phase chemical kinetics.

In this paper, the development of the wood pyrolysis model and then the new three-dimensional mathematical model to study flame spread over timber wall lining are described. Both the pyrolysis and burning of a vertical timber wall of a room and the turbulent flow, combustion and radiation in the room, are included. The predictions of the pyrolysis and fire models have been compared with the results of experiments. Excellent agreement has been achieved. The prediction of flashover behaviour of enclosure fire is also discussed.

INTRODUCTION

Flame spread and fire over cellulosic materials such as wood are important issues in fire safety design due to the frequent involvement of such materials in building fires and to the severity of the fires. Experimental studies to understand the mechanism of flame spread have been reported [1-4]. However, efforts to develop suitable mathematical models of flame spread in conditions of practical importance are not well developed. Many models, which are often classified as zone models, use empirical correlations derived from experiments. However the applications of these models are usually restricted to a particular set of fire scenarios and are, therefore, limited.

Field models based on CFD techniques have been used to study the behaviour of enclosure fires. Applications of CFD models for fire safety studies have been reported [5-8]. However, they did not take combustion into account but rather focused on a non-reacting gaseous flow in which the actual combustion processes were simulated by spatially distributed heat sources. Most importantly, these models did not include the pyrolysis of the solid which is the essential process governing the emission of combustible volatile pyrolysis products from the solid as the source of fuel. As a result, the emission of fuel gases from burning solids was not incorporated.

In order to model the complex behaviour of flame spread over cellulosic materials, a comprehensive field model, is required.

In this paper, we describe a new three-dimensional field model which includes the pyrolysis of the cellulosic material, emission of combustion gases from the material, gas phase combustion and feedback of heat from the burning region to the solid, causing further gasification. The model was used to predict the flame spread over cellulosic material such as timber wall lining and the subsequent fire development in enclosures until flashover. Excellent agreement was obtained.

WOOD PYROLYSIS MODEL

In the solid phase, multiple step first-order reactions are assumed for the pyrolysis of various active constituent of the wood becoming combustible gases. Evaporation of moisture in the wood is

assumed to be sufficiently rapid for the vapour to be in equilibrium. Energy and mass transfer in the solid occurs by thermal conduction and convection due to the movement of vapour, volatile gases and inert gases through the porous wood material. Two conservation equations for energy and mass were formulated. When these equations are transformed into a non-orthogonal curvilinear coordinate system ξ^i to cater for possible complex geometries in enclosures, they can be written in the following generalised form:

$$\sqrt{g}\,\frac{\partial\left(\rho_\phi^*\phi\right)}{\partial t}+\frac{\partial}{\partial\xi^i}\left(\beta_{\ell i}F_\phi^\ell\phi-\beta_{\ell i}\beta_{\ell j}\Gamma_\phi^\ell\,\frac{\partial\phi}{\partial\xi^j}\right)=\sqrt{g}\,S_\phi \qquad [1]$$

where ϕ denotes either temperature T_s or pressure P_s; superscript ℓ = 1, 2 or 3 denotes the directions along and across the grains to account for the anisotropic properties of wood, and the quantities ρ_ϕ^*, Γ_ϕ^ℓ, F_ϕ^ℓ and S_ϕ are listed in Table 1. $\beta_{\ell i}$, $\beta_{\ell j}$ and $\sqrt{g}$ represent the geometric coefficients and the Jacobian of the non-orthogonal curvilinear transformation.

TABLE 1. Coefficients and source terms for variables in the solid phase conservation equations

ϕ	T_s	P_s
ρ_ϕ^*	$\rho_s C_{ps}+\rho_m C_{pm}$	$\pi_g/\left(R_g T_s\right)$
Γ_ϕ^ℓ	λ_s^ℓ	$\alpha_s^\ell\left(\rho_v/M_m+\rho_g/M_g+\rho_i/M_i\right)/\left(\rho_v+\rho_g+\rho_i\right)$
F_ϕ^ℓ	$\dot{m}_g^\ell C_{pg}+\dot{m}_v^\ell C_{pv}+\dot{m}_i^\ell C_{pi}$	0
S_ϕ	$-\Delta H_{ev}R_{ev}-\Delta H_p R_p$	$R_{ev}/M_m+R_p/M_g$

The quantities C_{ps}, C_{pm}, ΔH_{ev}, and ΔH_p are the specific heats of virgin wood and water, and heats of evaporation and pyrolysis, respectively. The subscripts *g*, *v* and *i* denote volatile gas, vapour and the inert gas which is assumed to be present initially in the wood at ambient conditions.

In the wood pyrolysis model, the thermal decomposition of the cellulosic material and the evaporation of moisture are fully considered. The volatile gases and vapour are assumed to obey the ideal gas law with the gas and vapour densities assigned a dependence on porosity: The transfer of volatile gases and vapour is assumed to obey Darcy's Law with anisotropic permeability dependent on the orientation of the grains. The thermal conductivity and volumetric heat capacity of the pyrolysing wood vary linearly with char fraction. The permeability of the pyrolysing solid was described by an exponential function of the varying solid density as the wood progressively transforms to char [9-11].

All other thermodynamic and transport properties were allowed to vary linearly with temperature. Thermal swelling, shrinkage, surface regression and possible surface oxidation reactions of the virgin wood and char were neglected. The detailed development and formulation of the equations were reported in [9-11].

NUMERICAL SIMULATION OF PYROLYSIS OF WOODEN CUBE IN A FURNACE

To validate the 3-D wood pyrolysis model, it had been used to predict the pyrolysis of a wooden cube inside a furnace under various temperatures. The transformed governing equations were solved numerically using a control volume technique. Simulations were performed for the pyrolysis of wooden cubes of different initial moisture contents at furnace temperatures of 973 K and 1273 K. The activation energy and pre-exponential factor for the pyrolysis reaction of the single constituent have been adjusted to fit the measured mass loss history reported by Bonnefoy *et al.* [12]

The conservation equations were discretised using a control volume technique. The convection was modelled using a hybrid differencing scheme. The discretised equations were solved using the Strongly Implicit Procedure [13]. The 3-D pyrolysis model has been used to simulate pyrolysis of a wooden cube of dimensions 10 × 10 × 10 mm. Taking advantage of the cubical shape, only one-eighth of the cube was considered as the domain for simulation. Fig. 1 shows the computational domain with reference to the actual dimension of the cube. A total of 15 × 15 × 15 control volumes in the directions along and across the grains were used. A non-uniform mesh was used in the wood with the mesh concentrated adjacent to the heated external surfaces of the cube, to handle the steep gradients there. The boundary conditions and property values described in Yuen [9] were used.

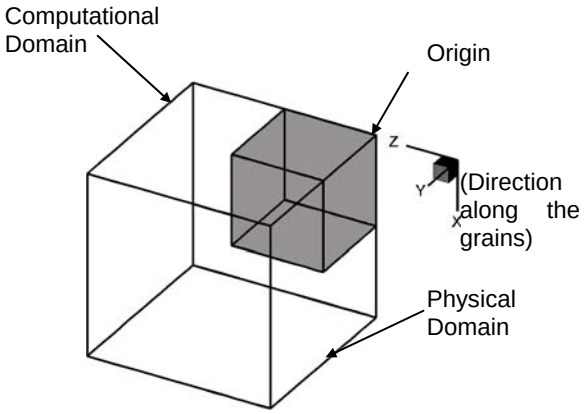

FIGURE 1. The physical and computational domain of the wooden cube (the wood grains are parallel to the *x*-axis)

COMPUTED RESULTS OF PYROLYSIS OF WOODEN CUBE IN A FURNACE

The model has been used to simulate the pyrolysis of a wet wooden cube with an initial moisture content X_0 = 9 % at furnace temperatures T_f = 973 K and T_f = 1273 K and the computed mass loss history has been compared with the experimental results on beech wood in [12]. Fig. 2 shows the good agreement achieved between the computed and experimental mass losses vs. time for the pyrolysis of the wooden cube. The result was obtained using an activation energy $E_p = 125$ kJ mole^{-1} and a pre-exponential factor $A_p = 1.25 \times 10^8$ s^{-1}.

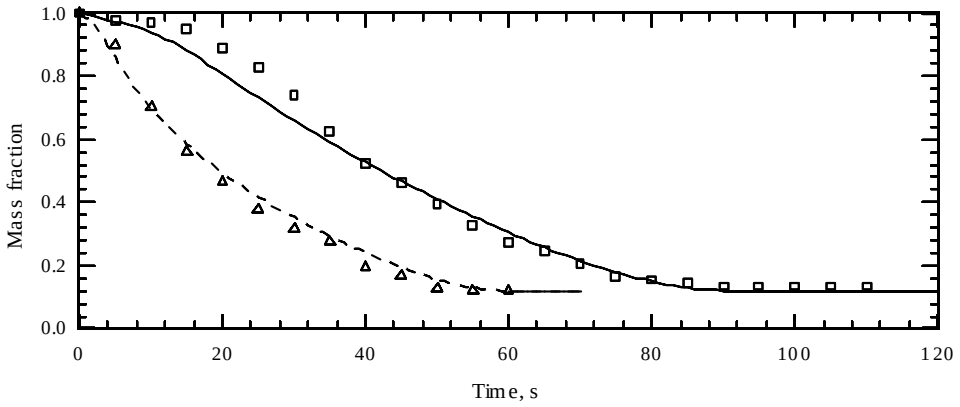

FIGURE 2. The computed mass fraction loss at the furnace temperature of 973 K (—) and 1273 K (- -), compared with experimental values at 973 K (□) and 1273 K (△) reported in [12]

A set of the computed transient results for the wet wood of X_0 = 9 % heated at a furnace temperature of 973 K are presented as an example and discussed in this paper.

Fig. 3 shows the isotherms and char fraction (ρ_c/ρ_w) and moisture content contours in the cube at t = 10 s for the furnace temperature of 973 K, on the y-z plane at x = 5 mm (mid-plane) and perpendicular to the direction of the grains. The char fraction contour of 0.02 (innermost) gives a good indication of the char front. The moisture content contours also indicate the advancement of the evaporation process in wood.

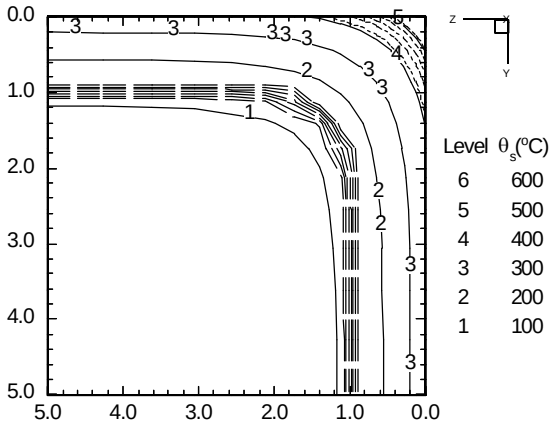

FIGURE 3. Isotherms (—) from 100 to 600 °C, char fraction contours (- - -) from 0.02 to 0.1 with step 0.02 and moisture content contours (– –) from 2 % to 7 % with step 1 % on y-z plane at x = 5 mm (mid-plane) at t = 10 s for T_f = 973 K and X_0 = 9 %

Fig. 4 shows a plot of isotherms together with the char fraction and moisture content contours in the cube at 10, 30, 60 and 80 s for the furnace temperature of 973 K, on the x-z plane at y = 5 mm (mid-plane). A wave-like propagation is observed for the isotherms from the external surfaces towards the centre of the cube as heating continues. The temperature gradients are weaker in the direction along the grains than across due to the relatively higher thermal conductivities in the former direction. On the other hand, the rate of advancement of the isotherms is found to be slower in the direction along the grains. This is due to the presence of large convective cooling as a result of internal flow of vapour and volatile gases in this direction, as reported previously [14]. The computed results fully illustrated the influences of anisotropy on pyrolysis processes in wood.

A 3-D mathematical model for the pyrolysis of wet wood has been developed which includes detailed considerations of the evaporation of moisture, anisotropic and variable properties, and pressure driven internal convection of gases in wood. It has been demonstrated that the current 3-D model for pyrolysis of wet wood can be used to describe the sophisticated chemical and physical processes involved in wood pyrolysis.

MATHEMATICAL MODEL FOR WOOD COMBUSTION AND FIRE

The model for the gas phase combustion consists of the three-dimensional, Favre-averaged equations of transport for mass, momentum, enthalpy and gas species concentration coupled with the wood pyrolysis model above was further developed. Turbulence is modelled using the two-equation κ-ε model, with the turbulent viscosity given by $\mu_t = C_\mu \rho \kappa^2/\varepsilon$ where ρ is the gas density. The effective viscosity μ_{eff} is obtained as the sum of the molecular and turbulent viscosities. In the κ and ε equations, production of turbulence due to buoyancy and the effect of thermal stratification of the turbulence dissipation rate are included in the G terms. The conservation equations in general form can be written

$$\frac{\partial(\rho\phi)}{\partial t} + \nabla \cdot (\rho \vec{u} \phi) = \nabla \cdot (\Gamma_\phi \nabla \phi) + S_\phi \qquad [2]$$

where ϕ represents the field variables; u, v and w are the velocities; κ and ε are the kinetic energy and dissipation of turbulence; h is the enthalpy; and Y_P, Y_F, Y_O, Y_{CO_2} and Y_{H_2O} are the mass fractions of combustible volatiles, propane fuel, oxygen, carbon dioxide and water vapour. Γ_ϕ and S_ϕ denote the diffusion coefficient and the source term respectively. Details of the equations are given in Table 2.

The closure constants for the κ-ε model are: c_μ = 0.09, c_1 = 1.44, c_2 = 1.92, c_3 = 1.44, σ_κ = 1.0 and σ_ε = 1.3. The Prandtl/Schmidt numbers are: σ_h = 0.7, σ_P = 0.7, σ_F = 0.7, σ_O = 0.7, σ_{CO_2} = 0.7 and σ_{H_2O} = 0.7.

The chemical reactions for the propane gaseous fuels and combustible volatiles inside the numerical cells are described by an Arrhenius expression [15] or by the mixing of the turbulent eddies containing intermittent species concentrations [16].

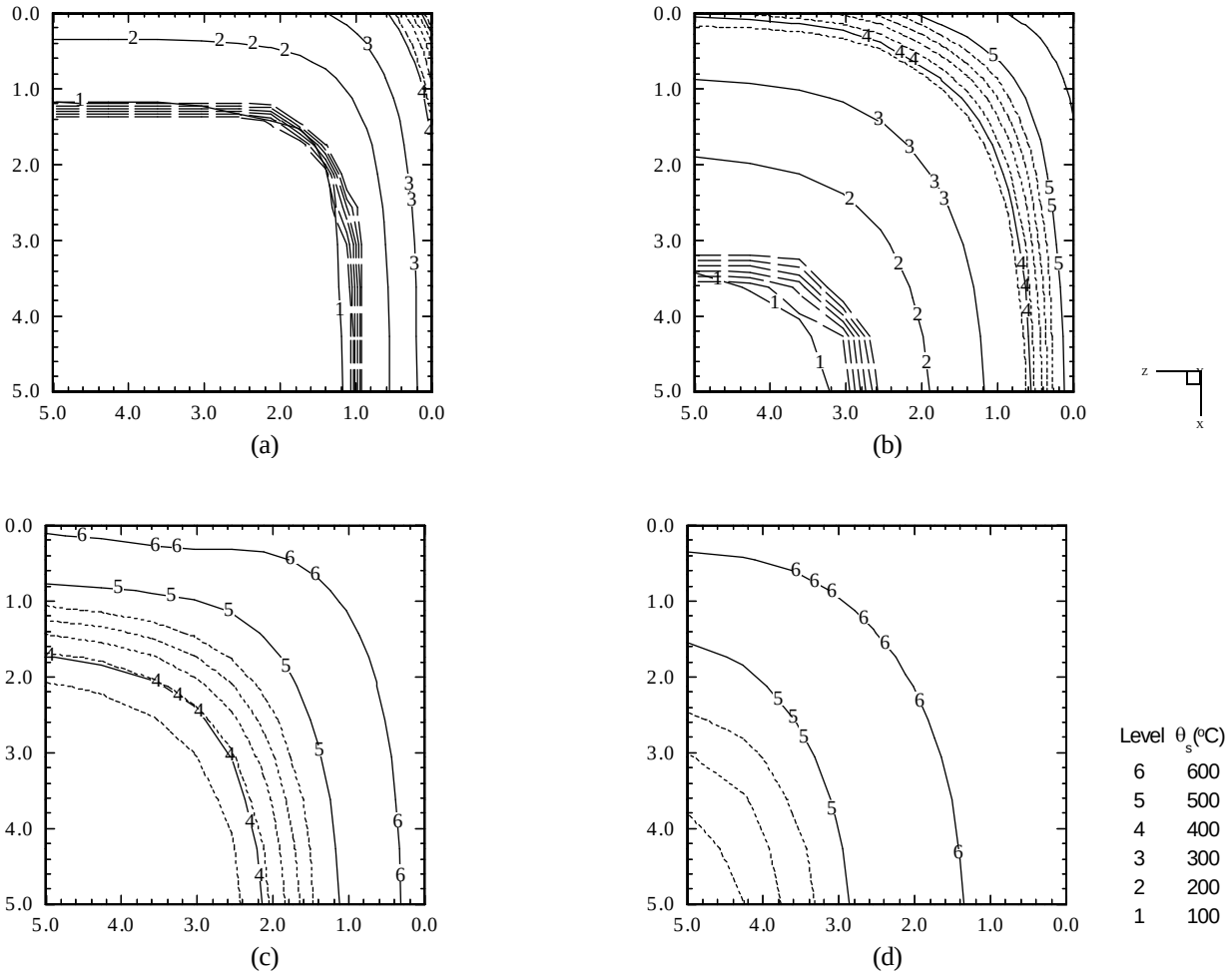

FIGURE 4. Isotherms (—) from 100 to 600 °C, char fraction contours (- - -) from 0.02 to 0.1 with step 0.02 and moisture content contours (– –) from 2 % to 7 % with step 1 % on *x*-*z* plane at *y* = 5 mm (mid-plane) at (a) *t* = 10 s, (b) *t* = 30 s, (c) *t* = 60 s and (d) *t* = 80 s for T_f = 973 K and X_0 = 9 %

TABLE 2. Transport equations for variable ϕ in the flow field

ϕ	Γ_ϕ	S_ϕ
1	0	0
u	μ_{eff}	$-\frac{\partial}{\partial x}\left[p+\frac{2}{3}\bar{\rho}\kappa+\frac{2}{3}(\mu_{\text{eff}})\left(\frac{\partial u}{\partial x}+\frac{\partial v}{\partial y}+\frac{\partial w}{\partial z}\right)\right]+\frac{\partial}{\partial x}\left((\mu_{\text{eff}})\frac{\partial u}{\partial x}\right)+\frac{\partial}{\partial y}\left((\mu_{\text{eff}})\frac{\partial v}{\partial x}\right)+\frac{\partial}{\partial z}\left((\mu_{\text{eff}})\frac{\partial w}{\partial x}\right)$
v	μ_{eff}	$-\frac{\partial}{\partial y}\left[p+\frac{2}{3}\bar{\rho}\kappa+\frac{2}{3}(\mu_{\text{eff}})\left(\frac{\partial u}{\partial x}+\frac{\partial v}{\partial y}+\frac{\partial w}{\partial z}\right)\right]+\frac{\partial}{\partial x}\left((\mu_{\text{eff}})\frac{\partial u}{\partial y}\right)+\frac{\partial}{\partial y}\left((\mu_{\text{eff}})\frac{\partial v}{\partial y}\right)+\frac{\partial}{\partial z}\left((\mu_{\text{eff}})\frac{\partial w}{\partial y}\right)-(\rho-\rho_o)g$
w	μ_{eff}	$-\frac{\partial}{\partial z}\left[p+\frac{2}{3}\bar{\rho}\kappa+\frac{2}{3}(\mu_{\text{eff}})\left(\frac{\partial u}{\partial x}+\frac{\partial v}{\partial y}+\frac{\partial w}{\partial z}\right)\right]+\frac{\partial}{\partial x}\left((\mu_{\text{eff}})\frac{\partial u}{\partial z}\right)+\frac{\partial}{\partial y}\left((\mu_{\text{eff}})\frac{\partial v}{\partial z}\right)+\frac{\partial}{\partial z}\left((\mu_{\text{eff}})\frac{\partial w}{\partial z}\right)$
κ	$\frac{\mu_{\text{eff}}}{\sigma_\kappa}$	$P+G-\rho\varepsilon$
ε	$\frac{\mu_{\text{eff}}}{\sigma_\varepsilon}$	$\frac{\varepsilon}{\kappa}c_1P+\frac{\varepsilon}{\kappa}c_3\max(G,0)-c_2\rho\frac{\varepsilon^2}{\kappa}$
h	$\frac{\mu_{\text{eff}}}{\sigma_h}$	S_{rad}
Y_P	$\frac{\mu_{\text{eff}}}{\sigma_P}$	$-R_P$
Y_F	$\frac{\mu_{\text{efff}}}{\sigma_F}$	$-R_F$
Y_O	$\frac{\mu_{\text{eff}}}{\sigma_O}$	$-\frac{\nu_O^F M_O}{\nu_F M_F}R_F-\frac{\nu_O^P M_O}{\nu_P M_P}R_P$
Y_{CO_2}	$\frac{\mu_{\text{eff}}}{\sigma_{CO_2}}$	$\frac{\nu_{CO_2}^F M_{CO_2}}{\nu_F M_F}R_F+\frac{\nu_{CO_2}^P M_{CO_2}}{\nu_P M_P}R_P$
Y_{H_2O}	$\frac{\mu_{\text{eff}}}{\sigma_{H_2O}}$	$\frac{\nu_{H_2O}^F M_{H_2O}}{\nu_F M_F}R_F+\frac{\nu_{H_2O}^P M_{H_2O}}{\nu_P M_P}R_P$

Radiation in fires is an essential part of fire modelling because of the presence of the combustion products which greatly augments the radiation heat transfer. The discrete ordinates method, an efficient and accurate method for calculating radiative transfer, is used [9].

NUMERICAL STUDY OF ROOM FIRE WITH TIMBER WALL

To further validate the wood combustion and fire model, it was used to predict the behaviour fire in an enclosure with a timber wall lining. The computed results were compared with the flame spread experiment performed in a room built according to the ISO/DIS 9705 (1990) standard. (see Fig. 5)

instrumented with Type K MIMS (Mineral Insulated Metal Sheathed) thermocouples with a 310 stainless steel sheath, an outer diameter of 1.5 mm and an unearthed junction. The propane sand burner was located at the bottom edge of the timber wall. The experiment was conducted with a heat release output of 40 kW for the first 5 minutes and 160 kW for a further 15 minutes. Video images were captured by a camera placed near the doorway.

In the computation, the non-uniform Cartesian grid is shown in Fig. 6; the grid concentration in the vicinity of the walls can be seen. A total of 40600 cells (only half the room was modelled due to symmetry). The solution domain reached beyond the doorway into an extended computational region, where constant pressure boundary conditions were applied. The boundary conditions and property values described in Yuen [9] were used.

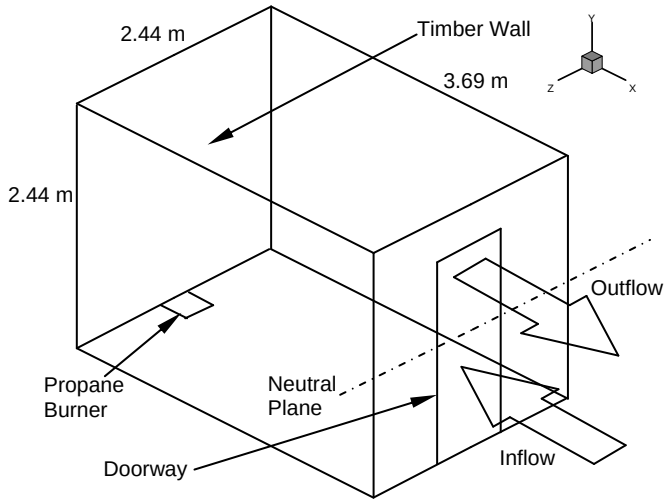

FIGURE 5. ISO/DIS 9705 (1990) standard room for fire tests

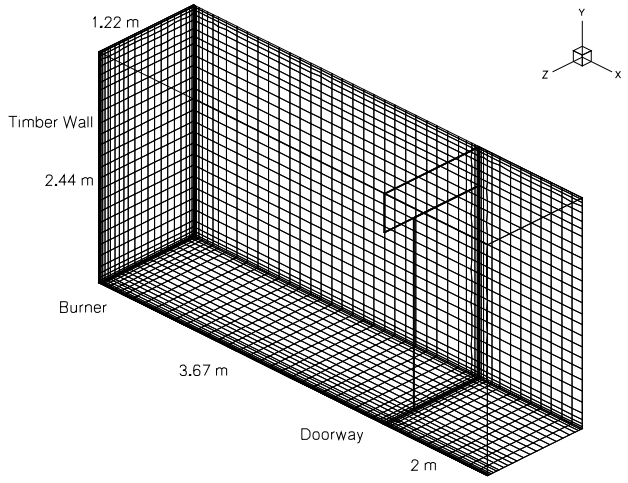

FIGURE 6. Solution grid

COMPUTED RESULTS AND PREDICTION OF ROOM FIRE BEHAVIOUR

The CFD model was used to simulate the flame spread and fire along the rear timber wall. The field plots of computed temperatures, velocities and mass fractions illustrate the transient development of the flame and fire until flashover. Experimental video images of the flame structures were also captured for comparison with the predicted results.

Figs. 7 to 8 show the computed temperature and velocity distributions over a *y*-*z* plane located at x = 0.029 m, at 441 and 690 s. Owing to the symmetric nature of this particular solution, it is sufficient to show only half of the elevation in the figures.

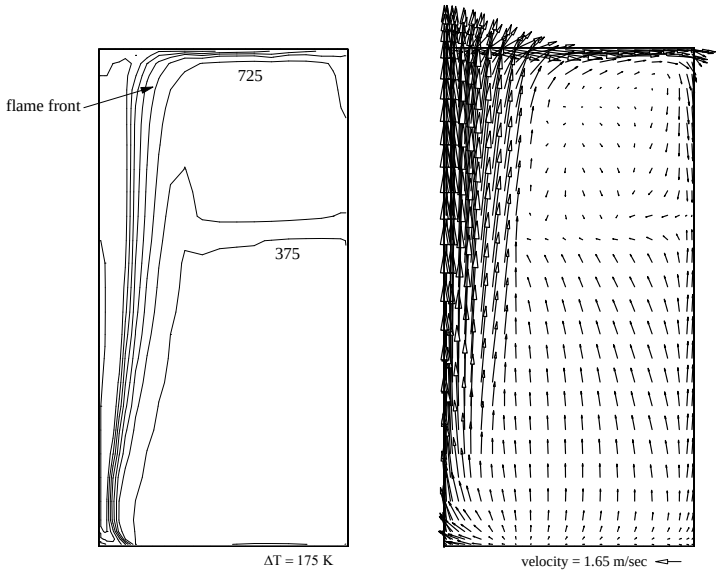

FIGURE 7. (a) Temperature and (b) velocity distribution immediately above the timber wall surface at 441 s

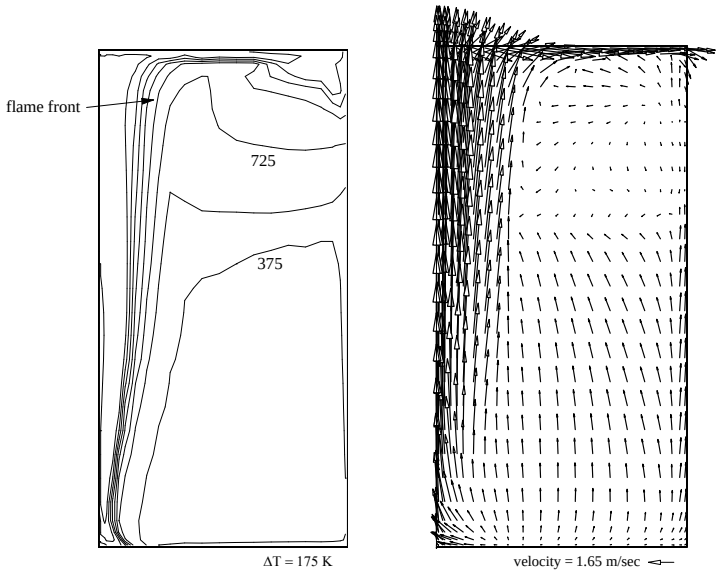

FIGURE 8. (a) Temperature and (b) velocity distribution immediately above the timber wall surface at 690 s

In Fig. 7(a), at 441s, the upward spreading flame reached the ceiling and was deflected horizontally, forming a ceiling jet. The jet then gave rise to a substantial increase of radiation and convection heat feedback to the unburnt timber underneath the ceiling causing the downward spread of the flame, Fig. 8(a) at 690s. Also, as rapid upward spreading was progressively gaining momentum, the horizontal spreads were intensifying, as indicated by the broadening of the burnt areas.

Figs. 9(a) and (b) show the temperature and velocity distribution in the symmetry plane z = 1.22 m at 742.5 s. The flames propagated away from the timber wall and covered the entire ceiling. Also, a tongue of flame was seen escaping from the room through the doorway. This conforms to the condition of flashover.

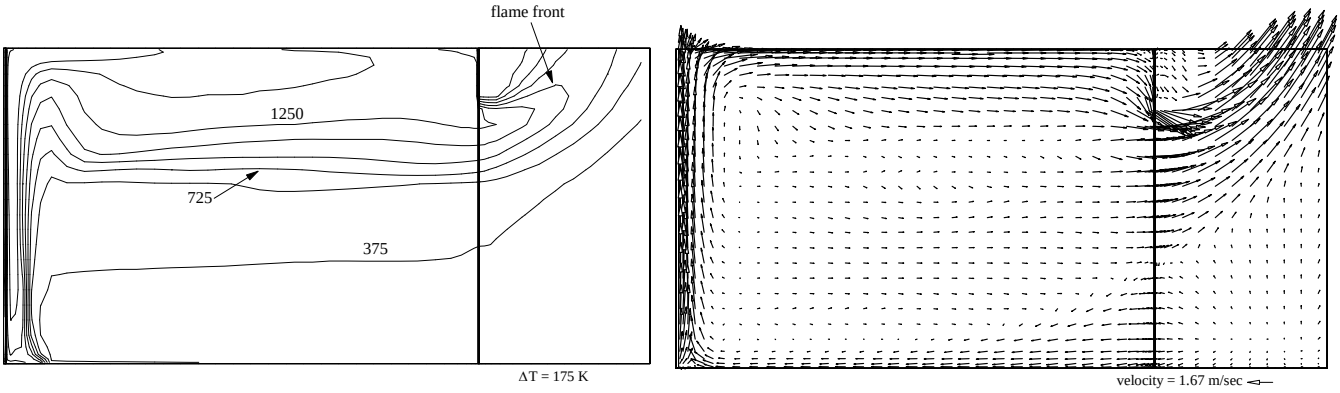

(a) (b)

FIGURE 9. (a)Temperature and (b) velocity distribution at symmetry plane at 742.5 s

Figs. 10(a) to (d) show video images taken during the experiment at 272, 441, 841 and 887 s. The computed flame structure shown in Fig. 7(a) corresponds extremely well to the experiment-ally observed shape. In Figs. 9(c) and (d), the video images show the onset and occurrence of flashover at 841 and 887 s, respectively. The computations, however, yielded an earlier time of 742.5 s in reaching this condition. This discrepancy could possibly be due to the assumption of single step reactions for the combustion of the propane fuel and combustible volatiles; another possibility is the assumption that the emissivity of the wall was assumed to be 1. Nevertheless, the prediction of fire growth and flame spread over the vertical timber wall in the enclosure made by the fire model correspond very well to the events seen during the experiment.

CONCLUSION

A 3-D CFD model for predicting flame spread and fire over cellulosic fuel in an enclosure has been developed and reported. The model comprises the governing equations for the turbulence, combustion, radiation and pyrolysis of the cellulosic fuel. The computed characteristics of the pyrolysis, flame spread and combustion phenomenon correspond very well to the experimental observations. It is recognised that the single step reaction schemes for combustion reaction in gas phase and also the emissivity of wood chosen can probably cause the discrepancy of the predicted time to flashover. Further developments of the model are thus needed.

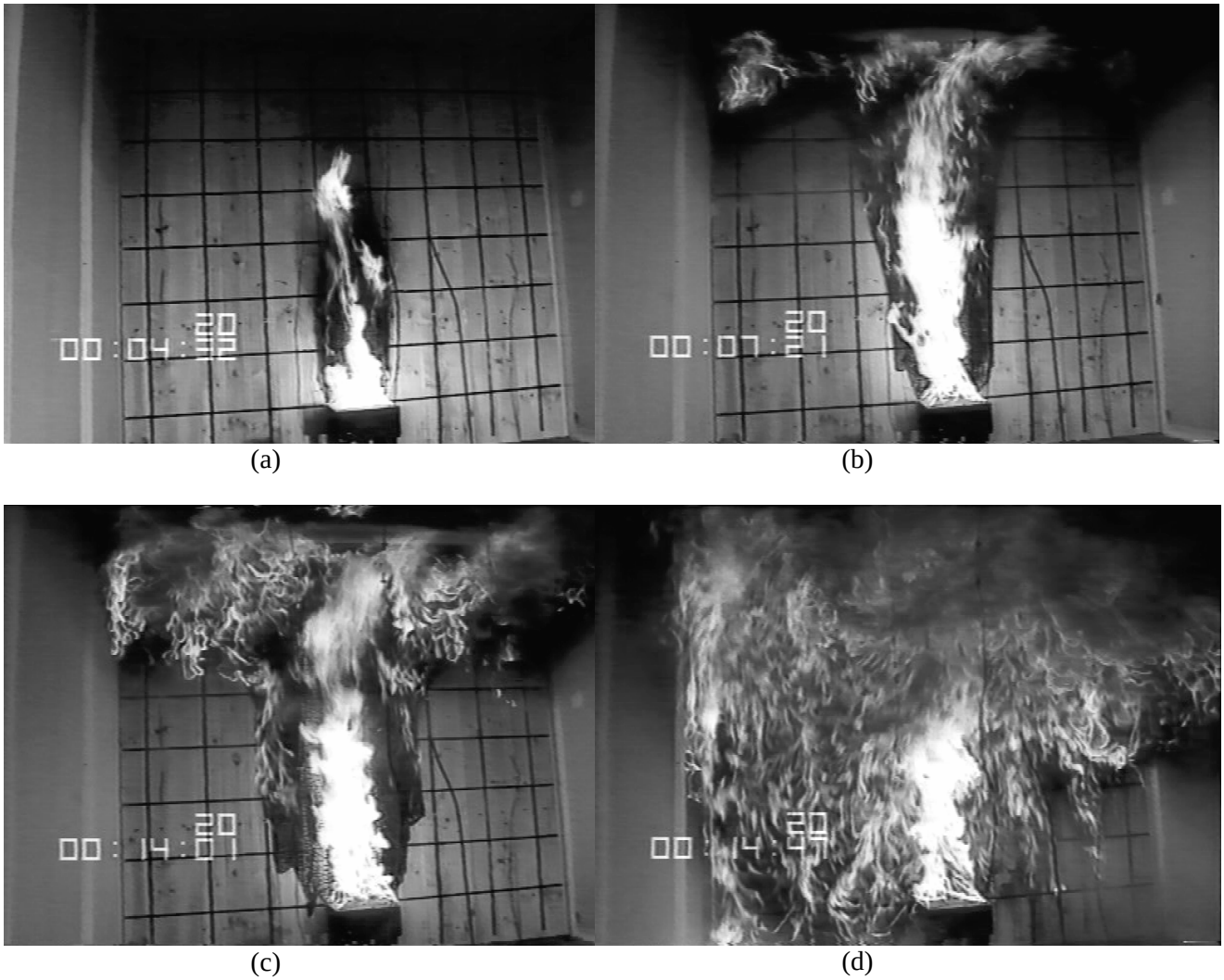

FIGURE 10. Video images of flame structures at (a) 272, (b) 441, (c) 841 and (d) 887 s

REFERENCES

1. Hirano, T., Noreikis, S.E. and Waterman, T.E., "Postulations of Flame Spread Mechanisms", Combustion and Flame, 22, 353-363, 1974.
2. Hirano, T., Noreikis, S.E. and Waterman, T.E., "Measured Velocity and Temperature Profiles near Flames Spreading over a Combustible Solid", Combustion and Flame, 23, 89-96, 1974.
3. Fernandez-Pello, A.C., Ray S.R. and Glassman, I., "Flame Spread in an Opposed Forced Flow : The Effect of Ambient Oxygen Concentration", 18th Symposium (International) on Combustion, The Combustion Institute, pp. 579-599, 1981.
4. Aterya, A., "Pyrolysis, Ignition and Fire Spread on Horizontal Surfaces of Wood", PhD Thesis, Harvard University, 1983.
5. Ku, A.C., Doria M.L. and Lloyd, J.R., "Numerical Modelling of Unsteady Buoyant Flows Generated by Fire in a Corridor", Proceedings of the Sixteenth Symposium (International) on Combustion, The Combustion Institute, pp. 1373-1384, 1976.
6. Hasemi, Y., "Numerical Calculation of the Natural Calculation in Fire Compartment", BRI Res. Paper, 1977.
7. Chow, W.K. and Wong, W.K., "A Study of the Fire Aspect of Atria in Hong Kong", Fire Safety Science - Proceedings of the Third International Symposium, pp. 335-344, 1991.
8. Markatos, N.C., Malin, M.R. and Cox, G., "Mathematical Modelling of Buoyancy-Induced Smoke Flow in Enclosures", Int. J. Heat Mass Transfer, 25, 63-75, 1982.

9. Yuen, R.K.K., “Pyrolysis and Combustion of Wood in a Cone Calorimeter”, PhD Thesis, University of New South Wales, Australia, 1998.
10. Yuen, R.K.K., Yeoh, G.H., de Vahl Davis, G. and Leonardi, E., “Modelling the Pyrolysis of Wet Wood – I. Three-dimensional Formulation and Analysis”, International Journal of Heat and Mass Transfer, 50, 4371-4386, 2007.
11. Yuen, R.K.K., Yeoh, G.H., de Vahl Davis, G. and Leonardi, E., “Modelling the Pyrolysis of Wet Wood – II. Three-dimensional Cone Calorimeter Simulation”, International Journal of Heat and Mass Transfer, 50, 4387-4399, 2007.
12. Bonnefoy, F., Gilot, P. and Prado, G., “A Three-dimensional Model for the Determination of Kinetic Data from the Pyrolysis of Beech Wood”, Journal of Analytical and Applied Pyrolysis, 25: 387-394, 1993.
13. Stone, H.L., “Iterative Solution of Implicit Approximations of Multidimensional Partial Differential Equations”, SIAM Journal on Numerical Analysis, 5, 530-558, 1968.
14. Di Blasi, C., “On the Influence of Physical Processes on the Transient Pyrolysis of Cellulosic Samples”, International Symposium on Fire Safety Science, pp. 229-240, 1994.
15. Westbrook, C.K. and Dryer, F.L., “Simplified Reaction Mechanisms for the Oxidation of Hydrocarbon Fuels in Flames”, Combustion Science of Technology, 27, 31-43, 1981.
16. Magnussen, B.F. and Hjertager, B.H., “On Mathematical Modelling of Turbulent Combustion with Special Emphasis on Soot Formation and Combustion”, 16th (Int.) Symposium on Combustion, The Combustion Institute, pp. 729-792, 1976.